

Spectral and non-linear optical properties of cyanine bases' derivatives of benzo[*c,d*]indole

O.I. Tolmachev^a, N.V. Pilipchuk^a, O.D. Kachkovsky^{a,*}, Yu.L. Slominski^a,
V.Ya. Gayvoronsky^b, E.V. Shepelyavyi^b, S.V. Yakunin^b, M.S. Brodyn^b

^a *Institute of Organic Chemistry NASU, Murmanskaya 5, 02660, Kiev-94, Ukraine*

^b *Institute of Physics NASU, pr. Nauki, 46, 03028 Kiev, Ukraine*

Received 9 December 2005; accepted 23 January 2006

Available online 26 May 2006

Abstract

The complex investigation of the cyanine bases, containing benzo[*c,d*]indole as residue group was carried out by linear and non-linear optical spectroscopic and quantum-chemical modelling methods. It was found that non-linear optical properties were more sensitive to the nature of the varied donor terminal group than the absorption spectra; the increase of the donor strength in indolenine, benzothiazole, quinoline, and pyridine causes an increase of the second and third hyperpolarizabilities by a factor of 3.5, which is qualitatively in good agreement with the experimental data.

© 2006 Published by Elsevier Ltd.

Keywords: Bases of cyanine dyes; Absorption spectra; Non-linear optical properties; Quantum-chemical calculations

1. Introduction

Donor–acceptor conjugated compounds are used intensively as non-linear optical materials [1–3]. Bases of cyanine dyes are the most suitable molecules for progressive investigation of the relationship between the structure and NLO properties. They are comparatively simpler and have high polarizable π -electron systems in which a donor and/or acceptor strength could be varied regularly and purposefully to obtain the optimal non-linear characteristics. Numerous advantages of this type of donor–acceptor molecules in comparison with classical merocyanines are connected with that the acceptor group in cyanine bases can be presented by nitrogen heterocycles with complicated and modified molecular topology, unlike acceptor residues in merocyanines containing, for example, one-coordinated oxygen atom [4,5].

On the other hand, linear and non-linear properties of the cyanine bases as derivatives of the well-known cationic cyanine dyes are readily interpretable and suitable for the establishment of the general regularities between the chemical constitution of donor–acceptor conjugated molecules and their NLO parameters. The most widely investigated compounds of this class are stable styryl bases (see review [6] and references therein). Upon excitation, they show intramolecular charge transfer process, especially, in polar solvents. This is why the cyanine bases possess an enormous potential for the molecular design of fluorescent probes [6] or non-linear optic materials [7]. As a rule, the studied bases have been constructed by a constant donor group (*p*-dimethylaminophenyl residue) and varying acceptor group. Until today, wide systematic study of cyanine bases with different donor residues has not been carried out.

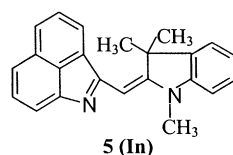
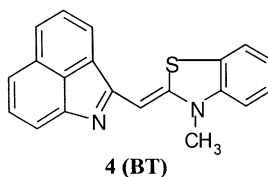
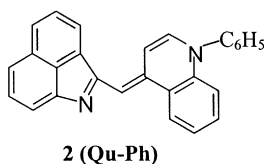
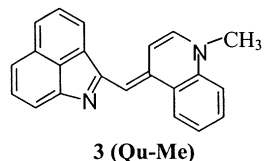
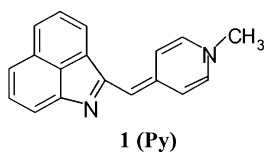
In the present paper, the results of the detailed study of the features of the electron structure, absorption spectra and some nonlinearities of the series of the cyanine bases with constant benzo[*c,d*]indole acceptor residue and various donor groups, basicity of which regularly changed, are considered.

* Corresponding author. Fax: +38 044 573 26 43.

E-mail address: iochkiev@ukrpac.net (O.D. Kachkovsky).

2. Materials and methodology

The bases of the cyanine dyes that were investigated are presented by the following structural formulas:



Absorption spectra were recorded on a spectrophotometer (Shimadzu UV-3100).

The laser beam self-action phenomena have been studied in the dioxane solution of the derivatives of cyanine bases by using the far field spatial profile analysis technique [8]. In the experiment, the sample was positioned far beyond the focal plane, 3 cm of the focusing lens, $f = 11$ cm, and was illuminated with a diverging Gaussian beam of a second harmonic Nd:YAG laser (wavelength 532 nm, duration time of a pulse 30 ps, repetition rate 3 Hz). For each laser shot, the light intensities were measured for the incident and transmitted laser pulses and for the pulse transmitted through an on-axis diaphragm in the far field (42.3 cm from the lens). The total and on-axis transmittances correspond to the photoinduced absorption and refractive index variation, respectively [9]. The diameter of

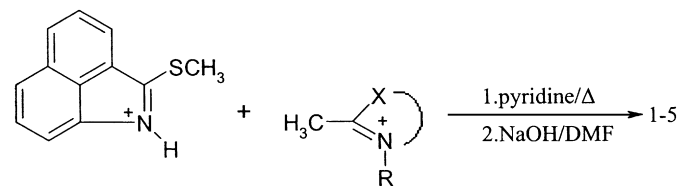
the beam spot was 0.17 mm at the sample in order to measure the NLO response in the range of 2–250 MW/cm² with a high signal to noise ratio. In addition, statistical averaging of about 10⁴ laser shots has been performed for measuring the intensity dependence of the NLO response for one sample. The measurements were performed at room temperature. The reversible character of the NLO response has been thoroughly controlled.

The equilibrium geometry of dye molecules in the ground state was optimized by the AM1 approximation (with the gradient of 0.01 kcal/mol). The 30 singly excited configurations were used upon calculation of the electron transition characteristics.

3. Results

3.1. Synthesis

The compounds **1–5** were synthesized as described earlier in the scheme [10].



3.1.1. Synthesis of 2-[(1-methylpyridin-4(1H)-ylidene)methyl]benzo[c,d]indole (1-Py)

A solution of 0.98 g (3 mmol) 2-methylthiobenzo[c,d]indolium iodide and 0.84 g (3.6 mmol) 1,4-dimethylpyridinium iodide in 3 ml of pyridine was heated at 110–115 °C (the temperature of oil bath) for 3 h and then cooled to the room temperature. In 3 h the precipitate was filtered off and washed by ethanol. The filter cake was dissolved in 10 ml of DMF at 100 °C and this solution was added to 50 ml of 5% aqueous solution of sodium hydroxide. The resinous product precipitated was levigated, filtered off, washed by water, and dried in vacuum desiccator over sodium hydroxide. The resulting product was recrystallized from toluene, yield 0.13 g (17%), decomposition point 208–209 °C. ¹H-NMR (DMSO-*d*₆), δ (ppm): 3.61 (s, 3H, N–CH₃), 5.91 (s, 1H, CH), 7.12 (d, $J = 6.6$ Hz, 1H, CH), 7.28–7.49 (m, 6H, CH), 7.55 (t, $J = 6.9$ Hz, 1H, CH), 7.80 (d, $J = 7.8$ Hz, 1H, CH), 7.86 (d, $J = 6.6$ Hz, 1H, CH). Elemental analysis of C₁₈H₁₄N₂—calculated: C, 83.69; H, 5.46; N, 10.85; found: C, 83.75; H, 5.41; N, 11.15.

3.1.2. Synthesis of 2-[(1-phenylquinolin-4(1H)-ylidene)methyl]benzo[c,d]indole (2-Qu-Ph)

2-[(1-Phenylquinolin-4(1H)-ylidene)methyl]benzo[c,d]indole (2-Qu-Ph) was prepared in the same way. The product was recrystallized from the mixture of toluene and hexane, yield 42%, m.p. 212–213 °C. ¹H-NMR (DMSO-*d*₆), δ (ppm): 6.83 (d, $J = 9$ Hz, 1H), 7.12 (s, 1H), 7.28–7.76 (m, 12H), 7.94 (d, $J = 7.8$ Hz, 1H), 8.35 (d, $J = 7.8$ Hz, 1H), 8.50 (d, $J = 7.8$ Hz, 1H).

Elemental analysis of $C_{27}H_{18}N_2$ —calculated: C, 87.54; H, 4.90; N, 7.56; found: C, 87.98; H, 4.71; N, 7.79.

3.2. Absorption spectra

The absorption spectra of cyanine bases investigated are presented in Fig. 1. One could see that in all the solvents the separated comparative intensive band is observed in the visible part which corresponds to only the first $\pi \rightarrow \pi^*$ electron transition. The higher transitions manifest themselves in the spectral region shorter than 400–450 nm. The positions of the maxima of the long wavelength bands of the dyes 1–5 are presented in Table 1.

Fig. 1 also shows that the position and shape of the bands are only somewhat sensitive to the nature of the solvents. Excepting methanol (Fig. 1a), in the polar acetonitrile (Fig. 1b), non-polar dioxane (Fig. 1c), and toluene (Fig. 1d), spectral bands are rather wide and structurally defined so that even the fine vibronic structure is observed, and $0 \rightarrow 1^*$ vibronic transition proves to be the most intensive.

It was found that solutions of the cyanine bases 1–5 are not stable. Upon exposure to air, the intensity of absorption bands of the base solutions decreases regularly. Study has shown that stability depends on the chemical constitution of the donor residue. So, the relative drop of the extinction coefficient (in %) within an hour is as follows: 15.71 (1, **Py**), 2.45 (**Qu**), 5.45 (**Qu-Ph**), 0.55 (**BT**) and 0.54 (**In**). After 2 weeks, all the solutions were practically discoloring.

Because of instability, only the freshly prepared solutions of the cyanine bases were used for the NLO measurements.

3.3. NLO properties

In Fig. 2 the total and on-axis transmittance dependencies versus input laser beam intensity are presented for the solution of the bases 2 with concentration 10^{-7} mole cm^{-3} . At the low-intensity range (3–10 MW/ cm^2) the sharp photoinduced darkening is accompanied by a positive refractive index variation, i.e. an increase of on-axis transmittance. The induced absorption saturated at 10 MW/ cm^2 and total transmittance keep the magnitude with low variation at about 0.5% up to high intensities. On the contrary, on-axis transmittances show the ranges with alternating refractive index variation.

The same dependencies are presented for the base 4 solution with concentration 5×10^{-8} mole cm^{-3} (Fig. 3). The total transmittance reveals sharp darkening with an intensity of up to 8 MW/ cm^2 , but at higher intensities of a photoinduced bleaching take place at two ranges. The on-axis transmittance has relatively strong variations at the high intensity region (150–250 MW/ cm^2).

3.4. Quantum-chemical data

In Table 2, the calculated energies of some of the lowest $\pi \rightarrow \pi^*$ electron transitions and dipole moments of the cyanine bases are presented while the wavelengths of the first

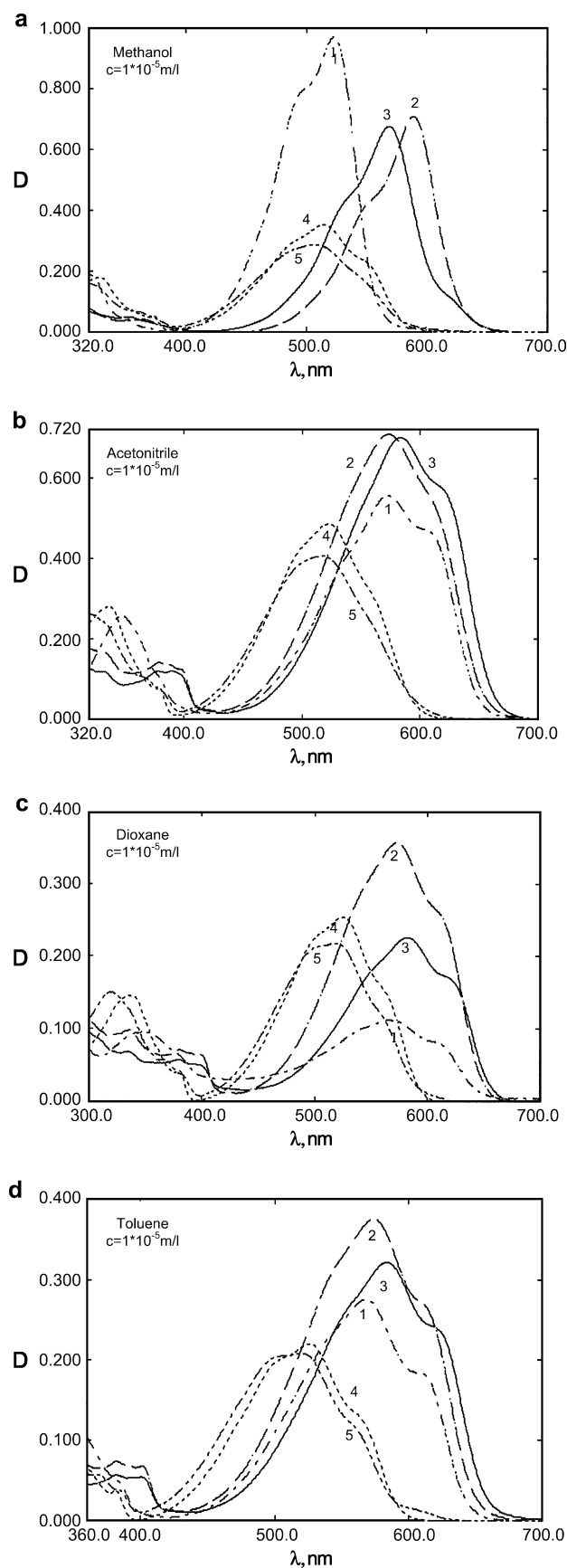


Fig. 1. Absorption spectra of bases 1–5 in different solvents.

Table 1

Absorption band maxima (λ_{\max}) and extinction (ϵ) as well calculated wavelength of the first electron transition of cyanine bases 1–5

Compound	Code	Dioxane		Toluene		Acetonitrile		Methanol		λ^{theor} , nm
		ϵ , 10^4	λ_{\max} , nm	ϵ , 10^4	λ_{\max} , nm	ϵ , 10^4	λ_{\max} , nm	ϵ , 10^4	λ_{\max} , nm	
1	Py	1.58	569	1.85	567	5.57	571	9.70	523	522
2	Qu-Ph	2.26	574	3.75	574	7.10	572	7.09	589	513
3	Qu-Me	3.57	582	3.21	583	7.01	584	6.76	569	531
4	BT	2.57	525	2.20	526	4.86	523	3.83	515	499
5	In	2.20	519	2.08	520	4.06	515	2.88	508	472

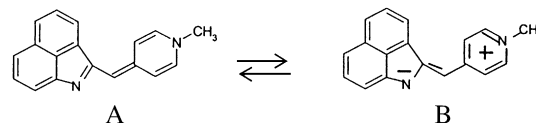
electron transition are tabulated in Table 1 together with the experimental band maxima, λ_{\max} . Comparison with the experimental data (in methanol) shows that there is an inconvergence to some extent between the calculated and spectral wavelengths; it is a typical imperfection of the AM1 approximation [11]. Of course, increasing the number of configurations upon the calculations of the energy of the excited state improves slightly the convergence between the calculated and spectral results, approximately on 10–15 nm. It was earlier shown [12] that better agreement between the band maxima and calculated wavelengths of the electron transitions can be reached in the PPP method; however, π -electron approximation (PPP and HMO) is not suitable to calculate state dipole moments because of σ -electrons being neglected. Meanwhile, the AM1 method reflects correctly the dependence of the energy of the electron transition on the molecular topology, in particular, chemical constitution of donor end groups; and hence, it can also be used for the calculation of such characteristics as state dipole moments, transitions moments and therefore for the estimation of the hyperpolarizabilities, i.e. non-linear optical properties.

4. Discussion

4.1. Electron asymmetry

Similar to other donor–acceptor conjugated systems, the cyanine bases 1–5 can be presented not only by a neutral structure, but also by a zwitterionic structure with the

separated negative and positive charges. For example, there are two main valence structures, A and B for the base 1:



The contribution of the structures depends on the so-called “basicity” of the end group X in the formulae 1–5, which corresponds to a donor strength of the terminal residue. It was shown by Brooker [13] that the heterocyclic compound used in this article can be positioned in the following way so that the basicity of heterocyclic residues decreases regularly: pyridine, quinoline, benzothiazole, and indolenine. Also, one could estimate quantitatively the donor strength of the donor end group by its topological index Φ_0 , which characterizes the ability of terminal residues to donate the π -electron density to the carbon atoms of the polymethine chain or, more correctly, to shift the modes of the frontier MOs from their positions in non-substituted polymethines [14]. It can be compared with the value ADBS (additional double bond stabilization) introduced by Brooker [13]. For the molecules with stable closed electron shell, the parameter Φ_0 magnitude is usually positive and falls within the interval $0^\circ \leq \Phi_0 \leq 90^\circ$. Then, the calculated indices Φ_0 for the heterocyclic residues above are presented in Table 3. One could see that the parameter Φ_0 decreases in the “Brooker series”: pyridine, quinoline, benzothiazole, and indolenine.

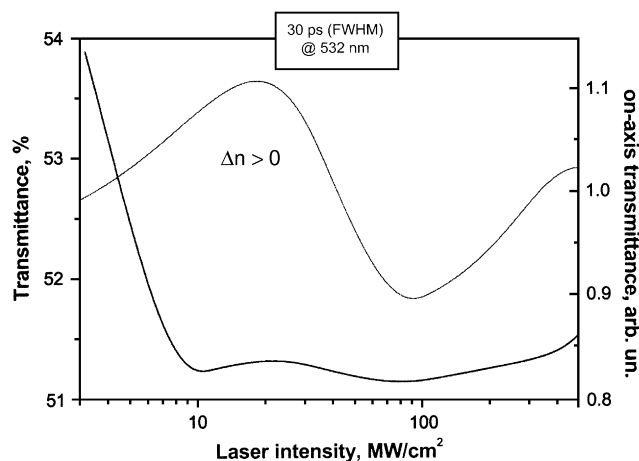


Fig. 2. Dependencies of transmittances of base 2 on intensity. Base 2, $\lambda = 532$ nm, $c = 10^{-4}$ mole/l.

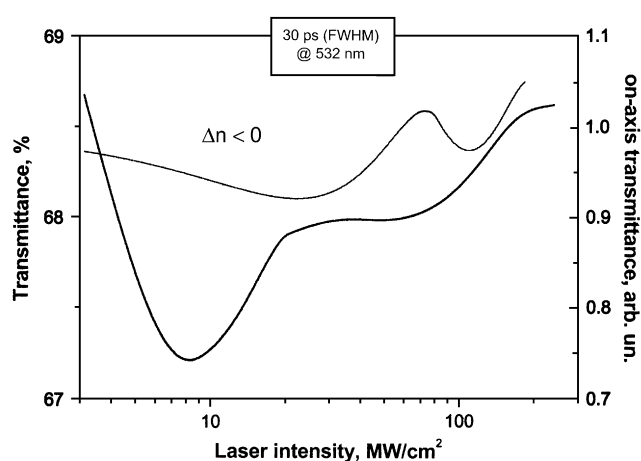


Fig. 3. Dependencies of transmittances of base 4 on intensity. Base 4, $\lambda = 532$ nm, $c = 5 \times 10^{-5}$ mole/l.

Table 2

Calculated characteristics of electron transitions in bases **1**–**5** (E is energy, μ_i is state dipole momentum, μ_g is transition dipole momentum and $\Delta\mu_i = \mu_i - \mu_0$)

Base	Transition	E , eV	μ_i , D	μ_{gi} , D	$\Delta\mu_i$, D
1	S_0	—	5.787	—	—
	$S_0 \rightarrow S_1$	2.367	9.011	9.024	3.224
	$S_0 \rightarrow S_2$	2.962	1.173	1.048	−4.614
	$S_0 \rightarrow S_3$	3.385	4.492	3.773	−1.294
	$S_0 \rightarrow S_4$	3.627	6.971	4.339	1.184
	$S_0 \rightarrow S_5$	3.787	3.872	1.135	1.915
2 (3)	S_0	—	4.001	—	—
	$S_0 \rightarrow S_1$	2.329	6.705	9.656	2.705
	$S_0 \rightarrow S_2$	3.171	3.239	1.403	−0.762
	$S_0 \rightarrow S_3$	3.322	2.384	3.783	−1.617
	$S_0 \rightarrow S_4$	3.503	3.744	0.54	−0.257
	$S_0 \rightarrow S_5$	3.724	3.606	2.4	−0.395
4	S_0	—	3.344	—	—
	$S_0 \rightarrow S_1$	2.477	5.937	8.108	2.593
	$S_0 \rightarrow S_2$	2.757	4.354	0.632	1.01
	$S_0 \rightarrow S_3$	3.416	2.742	2.903	−0.602
	$S_0 \rightarrow S_4$	3.533	4.895	1.182	1.551
	$S_0 \rightarrow S_5$	3.636	0.881	1.474	−2.463
5	S_0	—	2.411	—	—
	$S_0 \rightarrow S_1$	2.615	3.948	7.723	1.537
	$S_0 \rightarrow S_2$	3.42	2.87	3.362	0.459
	$S_0 \rightarrow S_3$	3.668	2.845	2.246	0.435
	$S_0 \rightarrow S_4$	3.684	2.233	2.56	−0.178
	$S_0 \rightarrow S_5$	3.758	3.784	1.559	1.374

Taking into consideration the physical meaning of the index Φ_0 as an ability to transfer an electron density, increase in the parameter Φ_0 should lead to an increase of the contribution of the valence structure B. This can be estimated by the alternation of the lengths Δl ; it is seen from Table 3 that the alternation is minimum for the base **1**, containing high basic pyridine residue and maximum for the base **5** containing the indolenine residue with the lowest index Φ_0 (the lowest donor strength).

The considerable alternation of the bond lengths is evidence of the asymmetry in an electron distribution in the chromophore, what becomes apparent, for example, in absorption spectra: the bases **1** (**Py**) and **2** or **3** (**Qu**) with the equalizing carbon–carbon bond lengths absorb in more long wavelength region than bases **4** (**BT**) and **5** (**In**) with the higher degree of the asymmetry (Fig. 1).

The electron asymmetry in the ground and excited states of the cyanine bases determines the magnitudes of the state dipole moments, μ_i . Table 2 shows that the momentum for the ground state, μ_0 , and for the first excited state, μ_1 , decreases regularly upon decreasing the strength of the donor

end group in the series: **1** (**Py**), **3** (**Qu**), **4** (**BT**) and **5** (**In**). Also, the same tendency is observed for the change of dipole momentum upon excitation, $\Delta\mu = \mu_1 - \mu_0$: 3.224, 2.705, 2.593 and 1.537 D, correspondingly. The last value, $\Delta\mu$, is one of the governing factors for the non-linear properties (see below, Section 3.3).

4.2. Electron transitions and absorption spectra

The separated spectral band observed in the visible part of the absorption spectra is connected with the first $\pi \rightarrow \pi^*$ electron transition involved mainly with the highest occupied MO and lowest unoccupied orbital. With the exception of base **1** containing the pyridine end group, all spectra exhibit the comparative wide band with the vibronic structure in any solvent, polar (CH_3CN , CH_3OH) and non-polar (dioxane and toluene). It seems likely that a substantial transformation of the shape of the long wavelength band in the methanol solution of the base **1** is caused by the formation of the hydrogen bonds between the hydrogen atom of the OH-group of the solvent molecule, CH_3OH , and the two-coordinated nitrogen atoms of the benzo[*c,d*]indole residue. In this case, the contribution of the zwitterionic valence structure B is maximum due to the highest donor strength (basicity) of the pyridine residue.

The vibronic transitions manifest themselves as shoulders on the spectral band. As a rule, the most pronounced vibronic structure is observed in the non-polar toluene. The approximate distance between vibronic transitions is found to be equal to $1100\text{--}1400\text{ cm}^{-1}$, which is close to the corresponding value for polymethine dyes and related compounds [13]. One could see from Fig. 1 that the $0 \rightarrow 1^*$ vibronic transition appears to be the most intensive (except, of course, piridocyanine base **1** in the methanol). Then, it enables the comparison of the positions of the absorption bands using their maxima (taking into consideration that the band maximum corresponds just to the most intensive vibronic transition, but not to the $0 \rightarrow 0^*$ transition).

4.2.1. Calculated and experimental data

The calculated and experimental wavelengths of the first electron transition for the cyanine bases are presented in Table 1. There exists a comparative agreement between both data. So, calculations predict bathochromical shift upon going from piridocyanine base **1** to the quinoderivatives **2** and **3** (+9 nm) and hypsochromical effect upon introducing benzo-thiazole or indolenine residues instead of the pyridine donor group (−23 and 50 nm), while the observed shifts of the band maxima are equal, +5, −44 and 50 nm, correspondingly. Also, it follows from Table 2 that the transition momentum, μ_{ij} , decreases in series: 9.656 D (**Qu**), 9.024 D (**Py**), 8.108 D (**BT**) and 7.723 D (**In**) what agreeing with the decrease of the absorption band extinction in the same order: 1.58×10^4 ; 3.67×10^4 ; 2.57×10^4 ; and 2.20×10^4 .

Table 3

Carbon–carbon bond lengths in the chain of bases **1**–**5**

Compound	R	Φ_0	l_1 , Å	l_2 , Å	Δl , Å
1	Py	76	1.4033	1.4000	0.0033
2 (3)	Qu-Ph (Qu-Me)	66	1.4063	1.4015	0.0048
4	BT	50	1.4105	1.3872	0.0233
5	In	40	1.4159	1.3790	0.0369

4.2.2. Solvation effect

Comparing the spectra of the bases in different solvents shows that the band maximum depends only slightly on solvent polarity, except the methanol in which hydrogen bonds could form. For example, going from the high polar acetonitril to the non-polar toluene is accompanied by the small bathochromic effect for the bases with the low basic donor groups, +3 nm (**BT**) and +5 nm (**In**), while for the base **1** with the most basic end group, the solvation effect is opposite in sign, –4 nm. The bases **2** and **3**, containing quinoline residue prove not practically sensitive to nature of solvent.

4.2.3. The higher electron transitions

Calculations have shown that energy of the second electron transition should be essentially greater so that the corresponding spectral bands are shifted hypsochromically, with respect to the first band, on 141 nm for the base (**Qu**), 115 nm (**Py**), 111 nm (**In**) and 51 nm (**BT**). It is seen from Table 2 that the transition dipole momentum of this electron transition, μ_{02} , is smaller than value μ_{01} for the first transition practically by a factor of 10. Taking into consideration that the oscillator strength is proportional to the square of the dipole momentum, $f \propto \mu_{ij}^2/E_{ij}$, where E_{ij} is a transition energy, then the intensities of the first and second electron transitions should differ hundred fold. Such conclusion agrees with the absorption spectra of the bases **1–5**; one could see from Fig. 1 that only the low intensive bands are observed in the spectral region at 350–430 nm.

Also, the calculated data show that the transition dipole moments μ_{ij} of next electron transitions increase somewhat with respect to the second transition, $S_0 \rightarrow S_2$, which is in good agreement with the observed spectra: absorption in the spectral region at 250–350 nm is more intensive. However, the spectral bands in the short wavelength part are unseparated and hence could not be in one-to-one correspondence with calculated energies of the higher electron transitions. Although, qualitative agreement between them can be observed, consequently, the calculated values E_{ij} and μ_{ij} are likely to be used for the theoretical estimation of the non-linear properties, in particularly, hyperpolarizabilities.

4.3. Non-linear optical properties

As it is seen from Figs. 2 and 3 the increase in the intensity of the incident light beam leads to an appearance of non-linear phenomena. So, the laser beam with the variable intensity by Z-scan technique causes firstly decreasing of the transmittance of the sample (the cyanine base solution) simultaneously with increasing of the refractive index, n . And thereafter, upon 20–30 MW/cm², the refractive index decreases to near 100 MW/cm².

It is known [4] that the change of a refractive index upon acting on the field of the laser light (a non-linear refractive index $n(J)$) is determined by the following formula:

$$n(J) = n_0 + n_2 J, \quad (1)$$

where J is intensity of the incident beam.

Table 4

Calculated hyperpolarizabilities of the bases **1–5**

Compound	Φ_0	β_0	D	N	T	γ_0
1	76°	281	1532	12 001	3526	–12 514
2 (3)	66°	279	1296	16 515	2706	–6943
4	56°	167	698	6825	927	–5200
5	40°	80	189	4775	1488	–3098

On the other hand, the value n_2 is directly connected with a third hyperpolarizability, $\chi^{(3)}$:

$$n_2 = 3\chi^{(3)}/8 \quad (2)$$

Figs. 2 and 3 show that non-linear characteristics depend on the chemical constitution of compounds.

On the molecular level, the macroscopic value of $\chi^{(3)}$ corresponds to the microscopic characteristic γ_{xxxx} , which can be calculated by the sum-over-states technique (SOS) derived from perturbation theory [4,5]. The simplified version of the SOS equations has been identified and provides useful model expressions for the second (β_0) and third (γ_0) hyperpolarizabilities:

$$\beta_0 [\text{model}] = 6\mu_{ge}^2 \Delta\mu / E_{ge}^2 \quad (3)$$

$$\gamma_0 [\text{model}] = 24 \left[\mu_{ge}^2 \Delta\mu^2 / E_{ge}^3 - \mu_{ge}^4 / E_{ge}^3 + \sum \mu_{ge}^2 \mu_{gk}^2 / E_{ge}^2 E_{gk} \right] = D - N + T$$

where the index g corresponds to the ground state, index e denotes the first excited state while the index k is related with the higher excitation and the value $\Delta\mu$ is the difference between the state dipole moments in the first excited and ground states, $\mu_e - \mu_g$. In the formula (4), the summation runs over a few excited states.

The calculated magnitudes of the parameters β_0 and γ_0 and its components D, N, T used 5 excited states ($k = 2–5$) for the investigated cyanine bases **1–5** and are listed in Table 4. One can see that increasing the donor strength estimated quantitatively by a topological index Φ_0 causes the regular increasing of the parameter β_0 by a factor of approximately 3.5, from 80 to 281 units.

The uniform regularity in the dependence of the value γ_0 on the basicity of the donor group is somewhat distorted, and hence calculation gives the maximum γ_0 for quinoderivatives (**Qu**) with the $\Phi_0 = 66^\circ$. This is because the base exhibits the lowest transition energy while the third hyperpolarizability is just more sensitive to the energy gap, as an E_{ge}^3

Table 5

Experimental non-linear characteristics of the bases **1–5**

Compound	λ_{max} , nm	TRA, cm/GW C = 10 ^{–4} mole/l	$\gamma \times 10^{-27}$, esu
1	569	860	5.2
2	574	520	4.2
4	525	336	–2.4
5	519	80	–0.8

(see the formula (4)). Also, one can see that the second term, N , gives the main contribution in the magnitude γ_0 . The small magnitude of the term T is connected with the relatively small transition moments, μ_{gk} , for the higher electron transitions (compare the corresponding data in Table 2).

The experimental non-linear characteristics are collected in the Table 5.

To compare correctly the experimental and calculated results, it is necessary to take into consideration the expressions (3) and (4) that become slightly modified when the dynamic NLO properties are estimated (as opposed to the static or model properties when a frequency of the incident beam is assumed to be equal to zero, $\hbar\omega = 0$).

The denominators in the formulae (3) and (4) should be changed to following terms, correspondingly:

$$(E_{ge} - 2\hbar\omega - i\Gamma_{ge})(E_{ge} - \hbar\omega - i\Gamma_{ge}) \text{ in Eq. (3)}$$

$$(E_{ge} - 3\hbar\omega - i\Gamma_{ge})(E_{ge} - 2\hbar\omega - i\Gamma_{ge})(E_{ge} - \hbar\omega - i\Gamma_{ge})$$

and

$$(E_{ge} - 3\hbar\omega - i\Gamma_{ge})(E_{ge} - \hbar\omega - i\Gamma_{ge}) \\ \times (E_{gk} + \hbar\omega - i\Gamma_{gk}) \text{ in Eq. (4)}$$

where Γ_{ge} is the damping factor associated with spectral band shape (≈ 0.10 – 0.15 eV).

5. Conclusion

The linear and non-linear spectral properties of the cyanine bases as donor–acceptor conjugated systems depend strongly on the asymmetry degree of electron structure in the ground and excited states. Providing the same acceptor end group (benzo[*c,d*]indole residue), asymmetry is determined by a donor strength or basicity of the another end group, which can be quantitatively estimated by its topological index Φ_0 . It is found that increasing the basicity in the

series indolenine, benzothiazole, quinoline, pyridine should increase the second and third hyperpolarizabilities by approximately a factor of 3.5.

The experimental data show the same tendency and are qualitatively in good agreement with the results obtained by the quantum-chemical calculations.

References

- 1 Bredas JL, Adant C, Tackx P, Persoons A, Pierce B. *Chem Rev* 1994;94:243–8.
- 2 Rettig W, Lapouyade R. In: Lacowich JR, editor. *Topics in fluorescence spectroscopy. Probe design and chemical sensing*, vol. 4. New York: Plenum; 1994. p. 109–21.
- 3 Tyutyulkov N, Fabian J, Mehlhorn A, Dietz F, Tadjer A. *Polymethine dyes. Structure and properties*. Sofia: St. Kliment Ohridski University Press; 1991.
- 4 Meyers F, Marder SR, Perry JW. *Introducing to the nonlinear optical properties of organic materials*. In: Interrante LV, Hampden-Smith MJ, editors. *Chemistry of advanced materials. An overreview*. New York/Chichester/Weinheim/Brisbane/Singapore/Toronto: Wiley-VCH, Inc.; 1998. p. 207–68 [Chapter 6].
- 5 Meyers F, Marder SR, Pierce BM, Bredas J-L. *J Am Chem Soc* 1994;116:10703–4000.
- 6 Rettig W, Rurack K, Szczepan M. *From cyanine to styryl bases – photophysical properties, photochemical mechanisms, and cation sensing abilities of charged and neutral polymethinic dyes*. In: Valeur B, Bredas J-L, editors. *New trends in fluorescence spectroscopy: applications to chemical and life sciences*. Berlin: Springer; 2001. p. 125–55.
- 7 Zbigniew R, Grabowski. Krystyna Rotkiewicz. *Chem Rev* 2003;103(10): 3899–4031.
- 8 Brodyn MS, Borshch AA, Volkov VI. *Refractive nonlinearity of wide-gap semiconductors and applications*. London: Harwood Academic Publishers; 1990.
- 9 Sheik-Bahae M, Said A, Wei T-H, Hagan D, Van Stryland EW. *J Quant Elect* 1990;4(760).
- 10 Fikcen GE, Kendall JD. *J Chem Soc* 1960:1537–41.
- 11 Kachkovski AD, Tolmachev AI, Slominskii Yu L, Kudanova MA, Derevyanko NA, Zhukova OO. *Dyes Pigments* 2005;64:207–16.
- 12 Fabin J, Zahradnic R. *Wiss Z Techn Univ (Dresden)* 1977;26:315–23.
- 13 Brooker LGS. *Rev Mod Phys* 1942;14:275–93.
- 14 Kachkovski AD. *Russ Chem Rev* 1997;66:647–64.